

Investigation of triple Cr-Ti-based nitride coatings depending on the graded transition layers

V. A. Chitanov*, L. P. Kolaklieva, T. M. Cholakova, R. D. Kakanakov

Central Laboratory of Applied Physics – Bulgarian Academy of Sciences, 61 Sankt Petersburg Bld., 4000 Plovdiv, Bulgaria

The results from investigation of the relation between the structure of the transition layers and nanohardness and adhesion of the triple Cr-Ti-based nitride coatings are presented in this article. The coatings were deposited on tool steel substrates at temperature of 140 °C and a nitrogen flow of 13 and 18 sccm. Two types of the coating composition, Ti/TiN/TiCrN and Cr/CrN/CrTiN were studied. Nanohardness of 21 GPa to 27 GPa and 22 GPa to 24 GPa was measured for Ti-based and Cr-based structures, respectively. The increase of the N₂ flow in the Cr-based samples has shown considerably improved adhesion to the substrates in comparison with the Ti-based ones. In both cases, the increase of reactive gas flow decreases the coefficient of friction to 0.14 for the Ti-based and to 0.10 for Cr-based structures. The optimal combination of nanohardness, adhesion and coefficient of friction was achieved for the Cr/CrN/CrTiN samples deposited at a nitrogen flow of 18 sccm.

Keywords: Hard coatings, Cr-Ti-N, transition layers, nanohardness, adhesion

INTRODUCTION

During the last years, the Cr- and Ti- based triple nitride coatings with graded transition layers deposited by unbalanced magnetron sputtering have attracted interest for implementation in the industry. The improved mechanical and tribological characteristics resulted from their structure are the main advantage ahead of the standard CrN and TiN coatings [1]. The enhanced mechanical properties of CrN based coatings with incorporated other metals allowed their wide application in the machining industry for improvement of the mechanical performance of stamping and machine components, molds and dies, tool holders and other industry tools [2, 3]. The industry interest is also increasing because of their high oxidation resistance [4]. The appropriate adhesion of the hard coatings is very important, feature, since these films are required to endure excessive loads when they are in industrial service, including cyclical, mechanical and thermal influences [5]. Therefore the triple coatings have to be designed in a way to have excellent coating-substrate adhesion, which ensures longer lifetime of the tools in harsh industrial environments. There are many tool materials limiting the coating deposition to temperatures lower than 200 °C. Such as carbon steels are preferred for industrial applications because of their lower price and specific applications. However, with the increase of the working temperature over 200 °C their hardness

decreases [6]. The adhesion of hard coatings on tool steel substrates is improved with increase of the working temperature [7, 8]. The achievement of optimal combination of excellent adhesion and enhanced nanohardness at deposition temperatures below 200 °C is a challenging technology task. The CrTiN hard coatings can be prepared by different techniques such as magnetron sputtering, ion beam assisted deposition, cathodic arc, and electron beam evaporation. Among these methods, the magnetron sputtering is one of the most widely used techniques to prepare films with large area uniformity and strong adhesion [9]. The Unbalanced Magnetron Sputtering is the most appropriate method for coating deposition at temperatures below 200 °C [10]. In the case of low deposition temperatures, the coating adhesion becomes a critical issue. It is assigned by the adhesion between the substrate and the first deposited metal layer as well as the cohesion between the adhesion metal layer and the graded transition layer. The investigation of relation between the structure of the transition layers and nanohardness and adhesion of the triple Cr-Ti-based nitride coatings deposited below 200 °C is presented in this article.

EXPERIMENTAL

The coatings were deposited on HSS substrates at temperature of 140 °C and nitrogen flow of 13 sccm and 18 sccm. Two structures, Ti/TiN/TiCrN and Cr/CrN/CrTiN, named Ti-based and Cr-based, respectively, were deposited by close field unbalanced magnetron sputtering (CFUBMS) in

* To whom all correspondence should be sent:
vchitanov@gmail.com

UDP 800-4 equipment (Teer Coatings, UK).

Fig.1 presents a scheme of the vacuum chamber used for deposition of the coatings. One Cr and one Ti targets arranged in an opposite configuration were used for deposition. The unused targets were protected by a shield or by an application of a low current of 0.5 A.

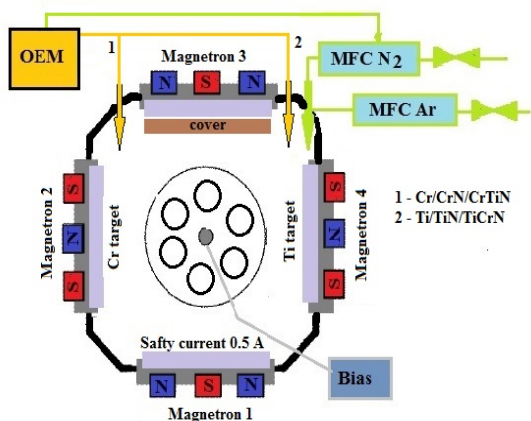


Fig.1. A vacuum chamber scheme of the UDP 800-4 equipment

Before the loading into the chamber, the specimens were ultrasonically cleaned in an alkaline solution, rinsed in deionised water and dried in a furnace. Prior the process start the chamber was evacuated to a base vacuum of 1.5×10^{-5} Torr. Ion cleaning in Ar plasma at a bias voltage of 500 V was performed for 30 min immediately before the coating deposition. The first Ti or Cr adhesion layer was deposited in Ar for 15 minutes. After that a transition layer of TiN or CrN was deposited by a gradually increased N_2 flow. During deposition, the nitrogen flow was controlled by OEM (Optical emission monitoring) with monochromator, tuned to the Ti (501 nm) or Cr peaks (421 nm). Two representative samples of each structure were chosen for investigation of the nitrogen flow effect on the properties of the transition and top layers. One transition layer was deposited at a nitrogen flow rate increased from 2 sccm to 13 sccm and the second one was obtained at a nitrogen flow rate risen from 2 sccm to 18 sccm. The increase was realized in 15 minutes. The internal stress between the transition layer and the active coating layer was reduced with deposition of a thin gradient TiCrN or CrTiN layer, realized by an increase of the Cr or Ti target currents respectively. The power of the Ti and Cr targets were kept a constant during deposition of the top TiCrN and CrTiN coating layers. The sputtering

process was controlled by the Ti and Cr target currents set in a Cr/Ti ratio of 0.7, because of their different reaction activity. The argon (Ar) flow was controlled by a mass-flow controller (MFC) and was kept a constant of 25 sccm during the process. The pulsed bias voltage was maintained at -70 V during deposition. The pressure during deposition varied between 1.6×10^{-3} and 1.9×10^{-3} Torr. The carousel rotated with 5 rpm. Thus, the only factor influenced the mechanical characteristics of coatings was the composition of the transition layers (Ti/TiN or Cr/CrN) and the applied nitrogen flow rate. The total thickness of the Ti-based coating was in the diapason $1.2 - 1.6 \mu\text{m}$, while of the Cr-based was between $1.5 - 2.0 \mu\text{m}$.

A Compact platform CPX- MHT/NHT – CSM Instruments, Anton Paar, Austria was used for characterisation of the mechanical parameters. The nanohardness was measured by a Berkovich indenter in the loading interval 0.01-500 mN. The Oliver and Pharr method was implemented for the calculations. Indentations with loads of 10, 15, 20, 50, 100 and 200 mN were made for the nanohardness study. The adhesion was qualified by a micro scratch test using a spherical Rockwell indenter with a radius of 200 μm . The coefficient of friction against a diamond indenter was also measured. A load progressively increased in the interval of 1 N to 30 N over a length of 1 mm was applied. The scratch velocity was 0.5 N/min.

The coating composition was studied by means of XPS and SEM/EDS analyses. The XPS spectra were acquired on a Kratos AXIS Supra photoelectron spectrometer using a monochromatic Al Ka source with an energy of 1486.6 eV. The base pressure in the analysis chamber was 5×10^{-8} Pa. The binding energies were corrected relative to the C1s peak at 285.0 eV. The elemental analysis was performed on JEOL JSM 6390 electron microscope, equipped with INCA Oxford EDS energy dispersive detector.

RESULTS

The load–displacement curves of the Ti-based coating at indentation loads of 10, 15, 50, 100 and 200 mN for the nitrogen flow rates of 13 and 18 sccm are presented in Fig.2.

The results show that the curves of both samples have the same slope and tendency. However, the curves corresponded to the sample prepared at a higher nitrogen flow are shifted to the bigger penetration depth implying lower nanohardness.

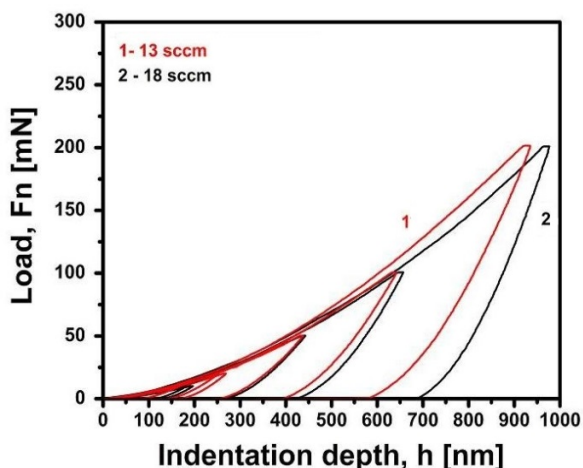


Fig.2. Load-displacement curves for Ti/TiN/TiCrN coating: 1) 13 sccm N₂ flow; 2) 18 sccm N₂ flow

This shift is more pronounced at bigger loads corresponded to penetration higher than 400 nm. Hence, this distinction could be attributed to the substrate than the coating.

The nanohardness H , modulus of elasticity E in dependence on the indentation depth h are presented in Fig.3.

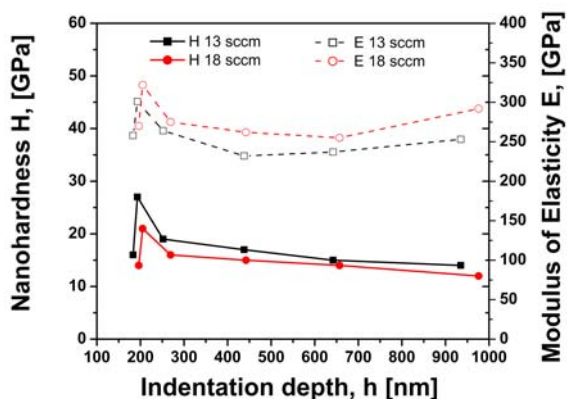


Fig.3. Dependence of the nanohardness and modulus of elasticity on the penetration depth of Ti/TiN/TiCrN coatings

A highest nanohardness of 27 GPa was measured at $h_{max}=193$ nm for the coating deposited at a N₂ flow rate of 13 sccm. The corresponded modulus of elasticity was 301 GPa.

The increase of nitrogen flow leads to decrease of the nanohardness to 21 GPa measured at h_{max} of 205 nm and a corresponding modulus of elasticity of 322 GPa. The nanohardness decrease at loads of 10 mN causes the surface contaminations and roughness [11]. With the indentation depth increase, the nanohardness decreased due to the influence of the substrate.

The load displacement curves as measured at 10, 15, 20, 50, 100 and 200 mN of the Cr-based structure are presented in Fig.4.

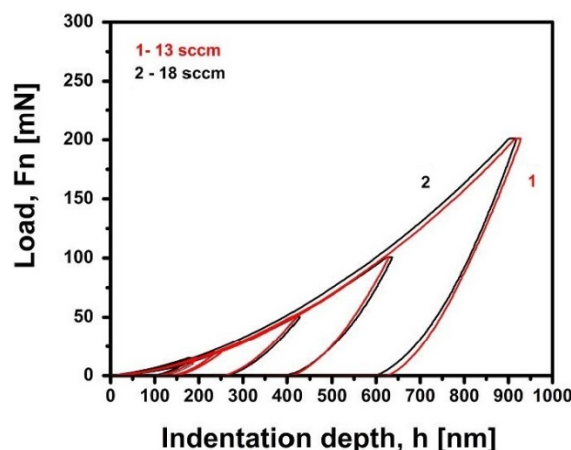


Fig.4. Load-displacement curves for Cr/CrN/CrTiN coating: 1) 13 sccm N₂ flow; 2) 18 sccm N₂ flow

The curves indicated an identical nanohardness for both N₂ flow rates. The maximum nanohardness measured at the indentation depth of 181 nm was 24 GPa and the modulus of elasticity was 380 GPa. The dependences of the nanohardness H and the modulus of elasticity E on the penetration dept, h for this structure are presented in Fig.5.

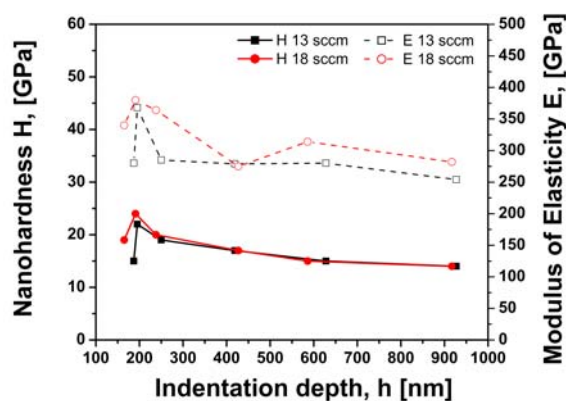


Fig.5. Dependence of the nanohardness and modulus of elasticity on the penetration depth of Cr/CrN/CrTiN coatings

It is seen that there is no difference in the curves corresponded to the both rates of the nitrogen flow. The slight nanohardness difference at a penetration depth of 200 nm is negligible.

Highest nanohardness of 22 GPa and a modulus of elasticity of 368 GPa were measured at a depth of 195 nm for the Cr/CrN/CrTiN coating obtained at 13 sccm nitrogen flow rate.

The study of the nanohardness revealed slight dependence on the nitrogen flow when OEM is tuned to the Ti peak, while the tuning to the Cr

peak does not cause significant dependence of the nanohardness on the nitrogen flow. This effect may relate to the higher titanium affinity to nitrogen than that of Cr atom ($\Delta H_{TiN} = -337.65$ kJ/mol, $\Delta H_{CrN} = -117.15$ kJ/mol). Therefore small changes of the nitrogen flow rate affect more pronounced nanohardness variation as the results for Ti/TiN/TiCrN coatings have shown. The highest nanohardness of 27 GPa and 24 GPa was measured for the Ti/TiN/TiCrN coating deposited at a 13 sccm nitrogen flow and for the Cr/CrN/CrTiN coating deposited at 18 sccm. Because the modulus of elasticity is an intrinsic property of the material, it does not depend essentially on the nitrogen flow rate.

The scratch test results of the Ti based coating with nitrogen flow rate of 13 sccm are shown in Fig.6. Four signals are presented in each graph: the applied normal force F_n , coefficient of friction μ , friction force F_t and acoustic emission AE.

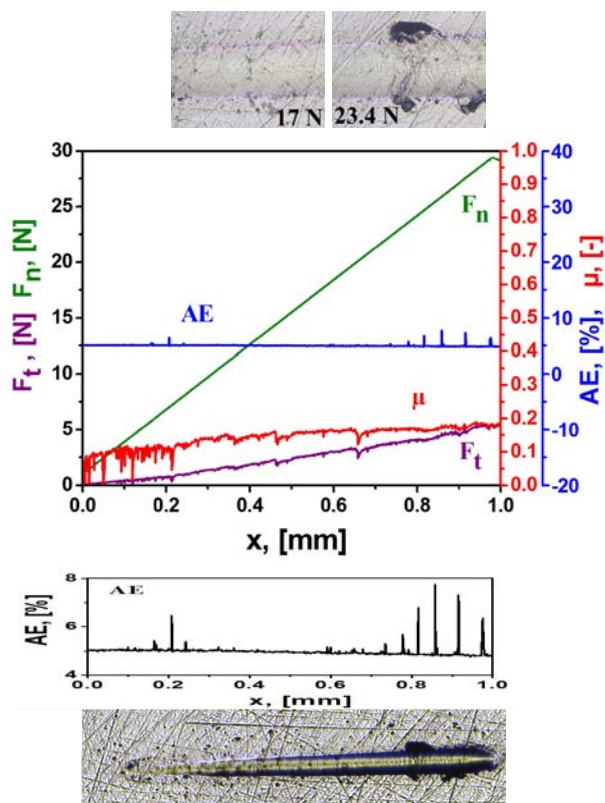


Fig.6. Scratch test results for the Ti/TiN/TiCrN coating at 13 sccm nitrogen flow: F_n - load force; F_t - friction force; μ - coefficient of friction; AE - acoustic emission; and a photo of the scratch test track

As it is seen, the coating exhibits a very good adhesion to the substrate. There was no delamination of the coating. At a load of 17 N a

small single crack was recognised, which related to small changes of the straight trends of F_t and μ . The AE signal has several peaks after 20 N, corresponded to rare small and short angular cracks implying weaker cohesion. Despite that, no chipping and spalling of the coating were appeared at loads up to 30 N. The measured coefficient of friction was 0.18.

The result of the Ti based coating obtained at a nitrogen flow of 18 sccm is presented in Fig.7.

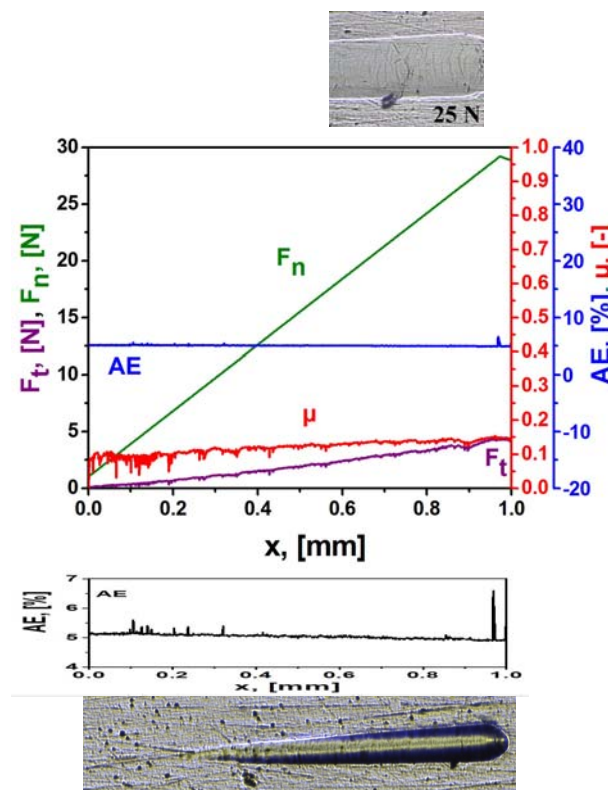


Fig.7. Scratch test results for the Ti/TiN/TiCrN coating at 18 sccm nitrogen flow: F_n - load force, F_t - friction force, μ - coefficient of friction, AE- acoustic emission; and a photo of the scratch test track

Again, a very good adhesion up to a load of 30 N was demonstrated. The improved adhesion up to 25 N could be evident from the scratch track and the trends of the friction force and acoustic emission. The latter was confirmed by the track visualization. A single-angle and several semi-spherical cracks were observed at loads over 25 N indicated with a small drop of the coefficient of friction and friction force. The measured coefficient of friction was 0.14.

The scratch test results of the Cr/CrN/CrTiN coating deposited at a nitrogen flow of 13 sccm are given in Fig.8. This coating also did not delaminate from the substrate. At the small load of 3 N there

was some drop of the coefficient of friction, most probably due to the surface defects. The small picks of the coefficient of friction and friction force signals at 14 N corresponded to thin semi-spherical cracks. The AE signal had not any features during the test. Few short angle cracks at the scratch edge at 27 N were identified. The adhesion of the coating during the scratch was very good. The coefficient of friction was 0.16.

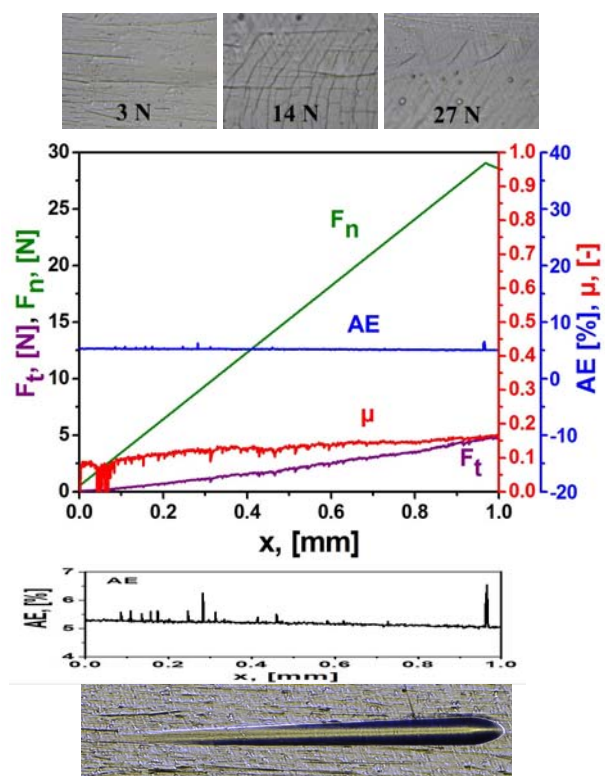


Fig.8. Scratch test results for the Cr/CrN/CrTiN coating at 13 sccm nitrogen flow: F_n - load force, F_t - friction force, μ - coefficient of friction, AE- acoustic emission; and a photo of the scratch test track

Excellent adhesion for loads up to 30 N was obtained for the Cr based coating deposited at an 18 sccm nitrogen flow. The results are presented in Fig.9.

The AE signal is smooth and no cracks were found during the test. The only one pick at the end of the AE signal could be attributed to the unloading process of the indenter and it did not correspond to a crack in the scratch track. There was no change in the trend of the friction force and the coefficient of friction. The measured value of the coefficient of friction was 0.1.

The dependence of the coefficient of friction on the nitrogen flow is presented in Fig.10.

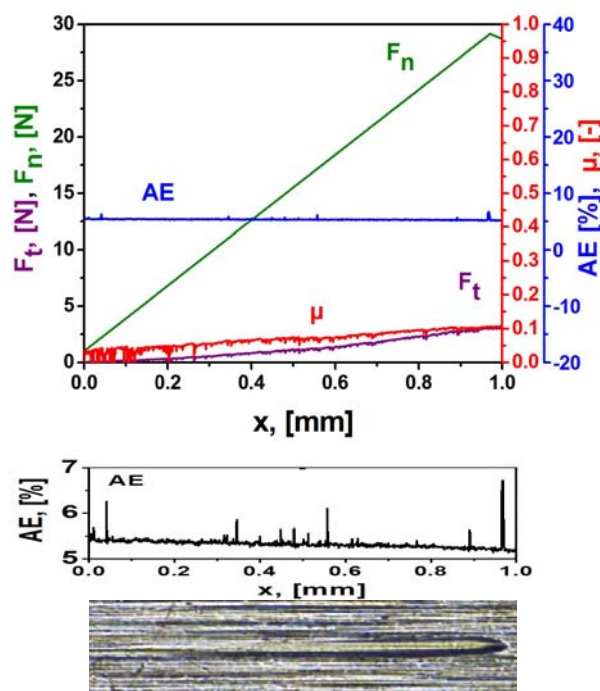


Fig.9. Scratch test results for the Cr/CrN/CrTiN coating at 18 sccm nitrogen flow: F_n - load force, F_t - friction force, μ - coefficient of friction, AE- acoustic emission; and a photo of the scratch test track

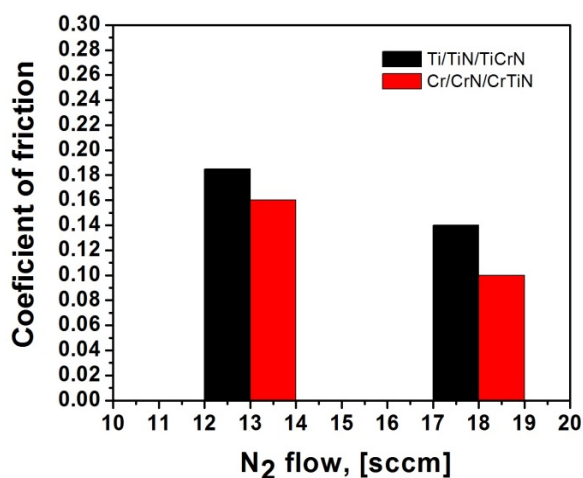


Fig.10. Coefficient of friction in dependence of the N₂ flow

The Cr-based coatings showed a lower coefficient of friction. It was evident that with the increase of the nitrogen flow the coefficient of friction for both structures was decreased. The lowest value of 0.1 had the Cr-based coating deposited at an 18 sccm flow.

The comparative study of the scratch results shown that the scratch resistance was very good with small non-essential cracks of the Ti-based coating. The Cr-based structures had better

scratch resistance because of the better adhesion strength of the CrN layer than the TiN one. This was confirmed by the excellent resistance to the progressive load from 1 to 30 N at 18sccm nitrogen flow.

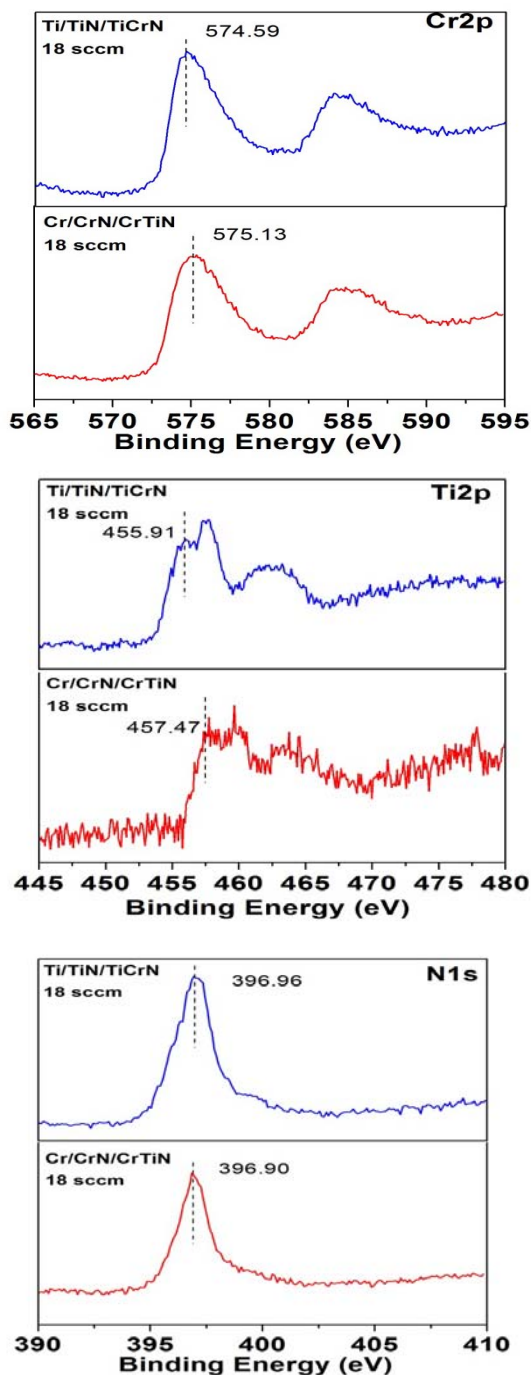


Fig.11. High resolution spectra of the Ti - based and Cr - based coatings

The chemical state and composition were obtained by XPS of the outmost coating layers.

High-resolution Cr (2p), Ti (2p), and N (1s) spectra are presented in Fig. 11. It is seen that the spectra of both coatings do not differ essentially in the shape. The Cr_{2p_{3/2}} peak is centered at 574.59 eV and 575.13 eV for Ti/TiN/TiCrN and Cr/CrN/CrTiN, respectively and possesses an asymmetric shape. The latter allows considering it as overlap of several peaks assigned to different chemical states according to reference data. Two of them could be assigned to CrN (BE 574.5 eV) and Cr₂N (BE 576.2 eV) in accordance with [12, 13]. It should be noted, that to the Cr (2p) peak could be contributed peaks between 576.1 and 576.6 eV assigned to Cr₂O₃ and CrO₂ [12, 14]. The oxygen contamination in a thin surface layer is very likely due to the air exposure of the coating. The third component which could be recognized in the Cr (2p) peak may relate to Cr (VI) state observed in binding energy range (578.1 - 579.8 eV) [15].

The positions of the Ti_{2p} peaks suppose the presence of TiN (BE 455.2 eV) [16] and titanium oxynitride (457.5 eV) and oxide (459.1 eV) [17]. The N_{1s} peak is centered at 396.96 eV in the Ti/TiN/TiCrN coating and at 396.90 eV in the Cr/CrN/CrTiN coating. This peak could be assumed as composed by peaks assigned to TiN at 395.7 eV [18] and two chromium nitrides, CrN (BE 396.7 eV) and Cr₂N (BE 399.7 eV) [19]. The results from the XPS analyses showed that the outermost layers of both coatings, Ti/TiN/TiCrN and Cr/CrN/CrTiN, obtained at the same technological regimes do not differ in a composition. They consist mainly of TiN, CrN and Cr₂N. The presence of oxynitrides and oxides was supposed due to the expose in air, as well. Hence, the difference of the mechanical properties results mostly by the different adhesion and transition layers than the coating composition.

The XPS analyses revealed that the outermost layer is composed by identical compounds when the Ti-based and Cr-based coatings were deposited at the same nitrogen flow.

Table 1. EDS elements analysis

Element	Ti/TiN/TiCrN – 18 sccm	Cr/CrN/CrTiN -18 sccm
	At. c. [%]	At. c. [%]
N	36.81	37.8
Ti	18.91	9.36
Cr	44.28	52.84

The element analysis from EDS investigation are shown in Tab.1. The nitrogen content in both

coatings was almost the same. The Ti was two times more in the Ti - based coating due to the Ti - based adhesion and transition layers. The Cr content was with small percentage higher in the Cr - based coating. It was prevailing over Ti and N in both structures.

CONCLUSIONS

Two coating structures Ti/TiN/TiCrN and Cr/CrN/CrTiN were developed for low temperature applications. The influence of the 13 sccm and 18 sccm nitrogen flow on the mechanical parameters was studied. It was found out that the nitrogen flow influenced mainly the transition layers responsible for the adhesion of the coating. The both structures were composed mainly from TiN, CrN and Cr₂N. The Cr-based coatings demonstrated better adhesion characteristics and lower coefficient of friction. The CrN further improved the mechanical properties of the transition layers. Lightly amended nanohardness was observed for the Ti based coatings deposited at lower N₂ flow. The increased N₂ flow improved the scratch resistance and reduced the coefficient of friction for both compositions. The Cr/CrN/CrTiN coating deposited at 18 sccm had the optimal mechanical characteristics and could be used for deposition on tools for industrial applications limited to temperatures of 200 °C.

REFERENCES

- [1] G. Zhang, P. Yan, P. Wang, Y. Chen, J. Zhang, The structure and tribological behaviors of CrN and Cr-Ti-N coatings, in *Applied Surface Science* **253(18)**, 7353-7359 (2007).
- [2] X. Zeng, S. Zhang, T. Muramatsu, Comparison of three advanced hard coatings for stamping applications, in *Surface and coating technology* **127**, 38-42 (2000).
- [3] S. Yang, K. Cooke, X. Li, F. McIntosh, D. Teer, CrN-based wear resistant hard coatings for machining and forming tools, in *Journal of Physics D: Applied Physics* **42(10)** (2009).
- [4] Y. Otani, S. Hofmann, High temperature oxidation behaviour of (Ti_{1-x}Cr_x)N coatings, in *Thin Solid Films* **281(1-2)**, 188-192 (1996).
- [5] R. Viana, A. Machado, Influence of adhesion between coating and substrate on the performance of coated HSS twist drills, in *Journal of the Brazilian Society of Mechanical Science and Engineering* **31(4)**, 327-332 (2009).
- [6] S. Jaypuria, Heat treatment of low carbon steel, Project report for Bachelor degree, India: Department of mechanical engineering, Nat. Institute of Technology, Rourkela, 2009.
- [7] M. Lufitha, Effect of substrate temperature on coating adhesion, Master thesis Canada: Department of Mechanical and Industrial Engineering, University of Toronto, 2001.
- [8] M. Al-Jaroudi, H. Hentzell, S. Gong, A. Bengston, The influence of titanium nitride reactive magnetron sputtering on hardened tool steel surfaces, in *Thin solid films*, **195(1-2)**, 63-76 (1991).
- [9] C. Paksunchai, S. Denchitcharoen, S. Chaiyakun, P. Limsuwan, Growth and Characterization of Nanostructured TiCrN Films Prepared by DC Magnetron Cosputtering, in *Journal of Nanomaterials*, 1-9 (2014).
- [10] M. Bao, X. Xu, H. Sun, J. He, Microstructure and Properties of Low Temperature Deposit Cr_xN Using Unbalanced Magnetron Sputtering, in *Key engineering materials* **353-358**, 1720 – 1723 (2007).
- [11] N. Demas, O. Ajayi, I. Shareef, Effects of Surface Contamination Layers and Roughness on the Determination of Mechanical Properties of Thins Films Using Nanoindentation, *Proc. of ASME/STLE International Joint Tribology Conference, Los Angeles, California*, 13-15 (2011).
- [12] I. Milosev, H. Strehblow, B. Navingek, XPS in the study of high-temperature oxidation of CrN and TiN hard coatings, in *Surface and coating technologies* **74-75**, 897 – 902 (1995).
- [13] A. Conde, A. Cristobal, G.Fuentes, T. Tate, J. Damborenea, Surface analysis of electrochemically stripped CrN coatings, in *Surf. & coating techn.* **201**, 3588 – 3595 (2006).
- [14] N. Heining, H. Jalili and K. Leung, Fabrication of epitaxial CrO₂ nanostructures directly on MgO(100) by pulsed laser deposition, in *Applied Physics Letters* **91**, 253102 (2007).
- [15] E. Unveren, E. Kemnitz, S. Hutton, A. Lippitz, W. Unger, Analysis of highly resolved x-ray photoelectron Cr2p spectra obtained with a Cr2O3 powder sample prepared with adhesive tape, in *Surf. & interface anal.* **36(1)**, 92 (2004).
- [16] A. Glaser, S. Surnev, F. Netzer, N. Fateh, G. Fontalvo, C. Mitterer, Oxidation of vanadium nitride and titanium nitride coatings, in *Surface Science* **601(4)**, 1153 -1159, (2007).
- [17] M. Thotiyl, T. Kumar and S. Sampath, Pd Supported on Titanium Nitride for Efficient Ethanol Oxidation, in *Journal of Physical Chemistry C* **114(41)**, 17934–17941 (2010).
- [18] D. Duartea, J. Sagasa, A. Sobrinhoa, M. Massi, Modeling the reactive sputter deposition of N-doped TiO₂ for application in dye-sensitized solar cells: Effect of the O₂ flow rate on the substitutional N concentration, in *Applied Surface Science* **269**, 55 -59 (2013).
- [19] A. Lippitz, T. Hubert, XPS investigations of chromium nitride thin films, in *Surface Coating Technologies* **200**, 250 – 253 (2005).